Indonesian Physical Review
Volume 09 Issue 01, January 2026
P-ISSN: 2615-1278, E-ISSN: 2614-7904

Twisted Intramolecular Charge Transfer in styrylpentafluorophenyl Aminopyrene: A DFT and TDDFT Study of Solvent Effects and Molecular Twisting Dynamics

Wafa Maftuhin[1*], Michael Walter[2]

[1]*Department of Physics, Faculty of Mathematics and Natural Sciences, Universitas Negeri Surabaya, Indonesia*
[2]*Freiburg Center for Interactive Materials and Bioinspired Technologies, University of Freiburg, Georges-Köhler-Allee 105, 79110 Freiburg, Germany.*

Corresponding Author's E-mail: wafamaftuhin@unesa.ac.id

Article Info

Article info:
Received: 29-07-2025
Revised: 30-10-2025
Accepted: 06-11-2025

Keywords:
DFT; TDDFT; Molecular conformation; solvent effect; TICT

How To Cite:
W. Maftuhin, M. Walter, "Twisted intramolecular charge transfer in styrylpentafluorophenyl aminopyrene: a DFT and TDDFT study of solvent effects and molecular twisting dynamics", Indonesian Physical Review, vol. 9, no. 1, p 39-48, 2026.

DOI:
https://doi.org/10.29303/ipr.v9i1.543

Abstract

Twisted intramolecular charge transfer is a key feature of donor–acceptor chromophores, significantly influencing their photophysical behavior. These processes are also central to the design of sensing and optoelectronic materials. In this study, we examine styrylpentafluorophenyl aminopyrene, which links a rigid pentafluorostyryl acceptor to a flexible N, N-dimethylaniline donor. Using density functional theory (DFT) and time-dependent DFT, we optimized ground and excited-state structures, mapped torsional energy surfaces, and explored solvent effects within a dielectric continuum model. The calculations indicate that the pentafluorostyryl unit remains locked in conjugation, while donor twisting through the dimethylaniline group drives the formation of a twisted intramolecular charge transfer (TICT) state. This mechanism reproduces observed solvent-independent absorption and solvent-sensitive fluorescence shifts of about 0.5 eV in polar media. The results place styrylpentafluorophenyl aminopyrene among donor-controlled twisted intramolecular charge transfer systems, while also highlighting how the structural asymmetry of a rigid acceptor and a flexible donor creates a single relaxation pathway. Such design principles can help guide the tuning of charge-transfer emission in functional dyes and related optoelectronic applications. In contrast to previously studied systems, styrylpentafluorophenyl aminopyrene reveals a distinctly donor-controlled mechanism reinforced by a rigid acceptor, establishing a new theoretical basis for predicting twisted intramolecular charge transfer behavior in asymmetric donor–acceptor chromophores.

Copyright (c) 2026 by Author(s). This work is licensed under a Creative Commons Attribution-ShareAlike 4.0 International License.

Introduction

Charge-transfer (CT) processes, in which an electron moves from an electron-rich donor to an electron-deficient acceptor, are central to photophysics and photochemistry. They underlie

fundamental natural processes, such as photosynthesis, and are key to the design of artificial light-harvesting systems, organic photovoltaics, and molecular electronics [1-3]. A common strategy to study CT is to construct donor–acceptor (D–A) molecules linked by a single bond. Upon electronic excitation, such systems may relax by twisting around this bond, leading to a twisted intramolecular charge transfer (TICT) state[4-10]. The TICT concept was first introduced through the dual fluorescence observed in 4-dimethylaminobenzonitrile (DMABN) [5,11],. In this model system, photoexcitation induces a rotation around the donor–acceptor bond, thereby decoupling their π *systems*. This twisting generates a charge-separated, polar excited state that emits at longer wavelengths than the locally excited state [3,12]. TICT has since been identified in numerous push–pull chromophores, and its properties are known to depend sensitively on solvent environment, molecular conformation, and substituent effects. Recent studies have highlighted the significant role of solvent polarity and basicity in stabilizing or destabilizing the TICT state, with implications for fluorescence wavelength, quantum yield, and excited-state lifetime [12-14]. Despite this progress, the detailed interplay between solvent stabilization and molecular design in activating TICT remains incompletely understood.

Pentafluorostyryl-aminopyrene (StyPy) provides a particularly compelling system for probing these effects. It incorporates an electron-donating N, N-dimethylaniline (DMA) unit and an electron-accepting pentafluorostyryl (PFS) group, both of which are directly conjugated to a pyrene core. This design differs from conventional D-A systems in which flexible linkers separate donor and acceptor; in StyPy, the intrinsic properties of the DMA and PFS units dominate the charge-transfer dynamics. Previous studies have shown that StyPy exhibits strong absorption in the far-red region, environment-sensitive emission, and molecular diode-like behavior in the solid state [15-16]. These characteristics make it an excellent model for studying the structural and electronic requirements of TICT, as well as for potential applications in optical sensing and photonic devices. In particular, two torsional pathways are available in StyPy: rotation of the PFS group relative to the pyrene backbone, and rotation of the DMA group. Determining which pathway dominates in excited-state relaxation is crucial for understanding the origin of its fluorescence properties. Experimental observations suggest polarity-dependent emission consistent with TICT formation. But a clear computational analysis of the competing torsional motions has been lacking. Moreover, while solvent effects have been widely studied in prototypical systems such as DMABN, their role in modulating TICT in StyPy has not been fully explored.

This investigation was therefore designed to address three key questions concerning the photophysical behavior of StyPy. First, which torsional pathway of the donor or the acceptor plays an important role in the formation of the TICT state? Second, how does solvent polarity influence the stability and emission energy of the twisted excited state? Third, to what extent does structural asymmetry, arising from a rigid acceptor and a flexible donor, enforce a single relaxation pathway? By addressing these questions, we test the hypothesis that limiting acceptor rotation while allowing donor leads to a predictable, donor-controlled mechanism for TICT formation. The insights gained from this work provide a clear understanding of how the molecular structure and solvent environment jointly influence the optical behavior of donor–acceptor systems.

To address these gaps, a comprehensive computational study was performed by combining density functional theory (DFT) and time-dependent DFT (TDDFT) with a continuum solvent model. Ground-state geometries were optimized and compared to experimental crystallographic data, while excited-state potential energy surfaces were mapped along the DMA and PFS torsional coordinates. Frontier molecular orbitals were analyzed to track charge redistribution between donor and acceptor units. Additionally, solvent effects were investigated across a wide range of dielectric environments, spanning from nonpolar to highly polar solvents.

Computational Methods

All calculations were performed with the GPAW package [17-18], using the projector augmented-wave (PAW) method on a real-space grid with a spacing of 0.20 Å. The smooth Kohn–Sham wavefunctions were represented on these real-space grids, while the electronic charge density was evaluated on finer grids with a spacing of 0.10 Å. The isolated molecule ($C_{27}H_{19}F_4NS$) consists of 52 atoms, featuring a pyrene backbone functionalized with a PFS acceptor and a DMA donor. The simulation box was extended to ensure at least 4 Å of vacuum around each atom to avoid spurious interactions. Ground-state geometries were optimized with DFT using the Perdew–Burke–Ernzerhof (PBE) generalized gradient approximation [19]. The PBE functional was selected for its balanced accuracy–cost ratio and well-established performance for conjugated π-systems. Structural relaxation was considered converged when the maximum residual force on any atom was below 0.05 eV/Å.

Optical excitation properties were calculated using TDDFT in Casida's linear-response formalism [20-21]. The number of unoccupied orbitals included in the response calculation was set equal to the number of occupied orbitals to ensure balanced representation of the excitation space. All transitions between Kohn–Sham orbitals within an energy range of 8 eV were considered in the linear-response calculations, which were verified to provide convergence for optical excitations below 3 eV. Vertical excitation energies and oscillator strengths were obtained from optimized ground-state structures, and excited-state minima were located by optimizing the lowest singlet (S_1) geometry. Potential energy surfaces (PES) were mapped by constrained optimizations of the dihedral angles associated with DMA and PFS rotation.

Solvent effects were modeled with the simplified continuum solvent model (CSM) [22], which represents the environment as a polarizable dielectric medium. Calculations were performed for the gas phase and solvents spanning a wide range of dielectric constants (ε_r): cyclohexane (2.02), toluene (2.38), chloroform (4.81), tetrahydrofuran (7.58), acetone (20.7), and dimethyl sulfoxide (46.8). Frontier molecular orbitals were analyzed to examine charge redistribution in S_0 and S_1 geometries. HOMO–LUMO gaps, orbital localization, and solvent-dependent spectral shifts were used to identify the dominant torsional pathway and quantify stabilization of the TICT state.

Results and Discussion

DFT optimized structures (Figure 1a) show that the pentafluorostyryl (PFS) group remains nearly planar with the pyrene backbone, while the N, N-dimethylaniline (DMA) unit is twisted by ~21°. This geometry is consistent with crystallographic data (26°) [23], confirming the accuracy of the computational model. The optimized C–N bond length between DMA and pyrene was 1.41 Å, consistent with conjugation but slightly longer than a typical aromatic C–N bond, reflecting partial decoupling. The pyrene backbone remains rigid and planar, as expected for aromatic

stabilization, while small deviations (<2°) occur at the PFS junction. The PES for PFS rotation (Figure 1b) indicates that in the excited state (S_1), the energy rises by ~0.8 eV as the dihedral approaches 90°. The minimum remains near 0°, showing that PFS twisting does not contribute to TICT formation or to significant changes in fluorescence spectra. This behavior differs from that of classic acceptor-twisting systems, such as DMABN and its derivatives, where the twisting of the benzonitrile unit directly leads to charge separation [5]. In StyPy, the strong electron-withdrawing nature of the PFS unit favors planarity with the pyrene backbone, maintaining π-conjugation. Similar rigidity has been observed in cyanoacrylate-based push–pull dyes, where the acceptor unit resists twisting and the donor governs TICT dynamics [13], [24]. Thus, the PFS moiety acts as a fixed acceptor, leaving DMA twisting as the only viable relaxation pathway.

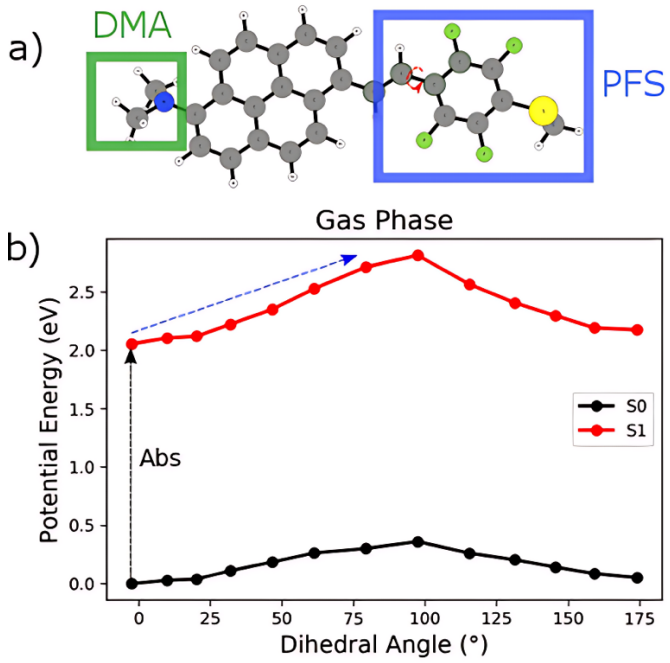

Figure 1. a) DFT optimized ground-state geometry of StyPy, showing planar alignment of the PFS acceptor with the pyrene backbone and a ~21° twist of the DMA donor. White = H, gray = C, green = F, yellow = S, Blue = N, and the red circular line indicates the torsional coordinate used for PES scanning. b) PES scan of PFS rotation in the first excited singlet state (S_1).

In contrast, PES scans of DMA rotation (Figure 2) reveal stabilization of S_1 at a near-orthogonal (~90°) geometry. This conformation corresponds to a TICT state, in which donor–acceptor orbital overlap is strongly reduced. The twisting process is thermodynamically favorable, enabling charge separation and resulting in an increased dipole moment. The timescale of TICT formation in related pyrene-DMA systems has been reported in the sub-picosecond to picosecond regime [25]. Suggesting that rotation around the DMA–pyrene bond is nearly barrierless in S_1. This kinetic contrast between donor and acceptor torsions indicates that donor rotation provides the dominant and fastest route toward TICT formation, while the PFS rotation remains hindered by its ~0.8 eV barrier. Comparable donor-driven TICT has been reported in chalcone derivatives [3], where the rotation of dimethylamine leads to pronounced solvent-dependent emission. Experimental fluorescence redshifts in polar solvents [15], [25] confirm this mechanism,

establishing DMA twisting as the dominant pathway for TICT formation in StyPy, while PFS remains inactive.

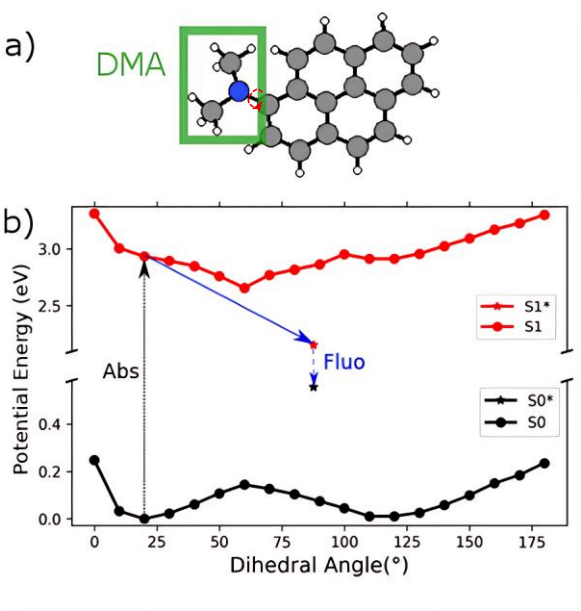

Figure 2. a) Optimized ground-state configurations of the PyDMA molecule. b). PES scans for DMA torsion in the PyDMA. In the ground state (S_0), the energy minimum occurs near 21°, but in the first excited singlet state (S_1), a second minimum emerges near 90°, corresponding to a TICT geometry. The asterisk (*) symbols denote geometries optimized in the excited state, representing relaxation following vertical excitation.

To illustrate this mechanism, Figure 3 shows a schematic energy diagram that summarizes the relaxation from the locally excited (LE) state to the TICT state. The diagram highlights the key features of the process: the barrierless rotation of the donor, the barrier-limited rotation of the acceptor, and the relative stabilization of the TICT configuration. This representation connects the calculated potential energy surfaces with the proposed kinetic pathway, providing a straightforward view of how structural asymmetry influences the TICT dynamics in StyPy.

Frontier molecular orbitals (FMOs) clarify the electronic changes driving TICT (Figure 4). In the ground state (S_0), the HOMO is delocalized across DMA and pyrene, while the LUMO is localized on pyrene. In the twisted S_1, the HOMO localizes on DMA and the LUMO remains on pyrene, consistent with charge transfer. The HOMO–LUMO gap decreases from 2.24 eV in S_0 to 1.6 eV in S_1. The higher HOMO energy reflects the enhanced electron-donating ability of DMA, while the lower LUMO energy strengthens electron acceptance by pyrene. Together, these shifts confirm efficient donor–acceptor charge separation in the twisted state. The oscillator strength (f) of the $S_0 \rightarrow S_1$ transition was calculated as 0.18, consistent with a moderately allowed HOMO–LUMO transition. Upon twisting, orbital overlap decreases, and *f* is slightly reduced (0.14), indicating weaker transition dipole strength. Similar reductions in oscillator strength upon TICT formation have been documented in the push–pull systems [3], [25], where orbital decoupling leads to diminished fluorescence quantum yield.

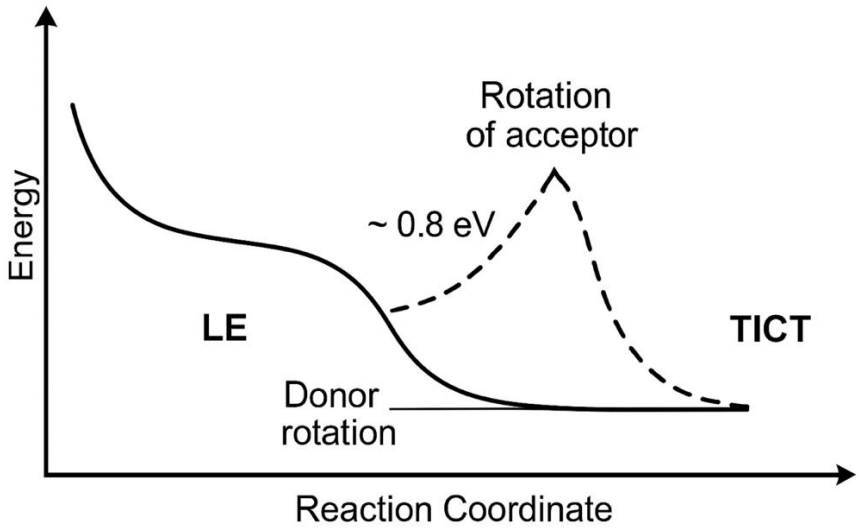

Figure 3. Schematic energy-level diagram illustrating the relaxation mechanism from the locally excited (LE) state to the TICT state of styrylpentafluorophenyl aminopyrene. The donor (DMA) torsional motion proceeds through a nearly barrierless pathway, whereas the acceptor (PFS) rotation requires overcoming a ~ 0.8 eV barrier.

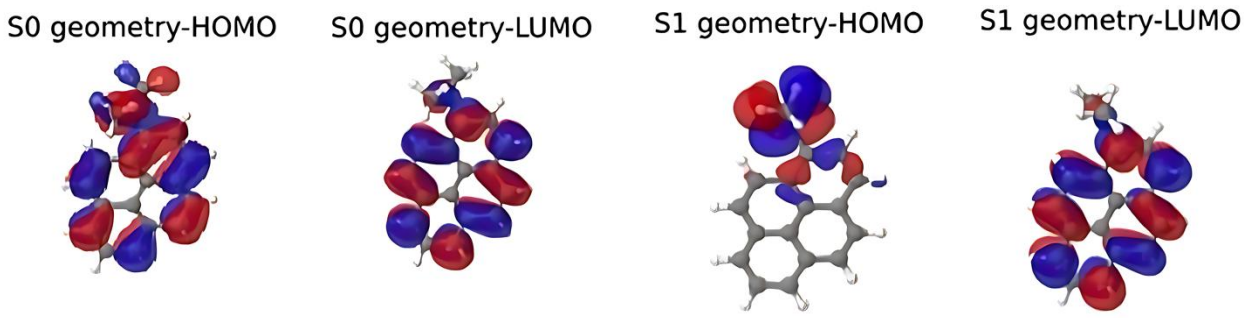

Figure 4. Frontier molecular orbitals of StyPy. In the ground state (S_0), the HOMO extends over DMA and pyrene, while the LUMO is localized on pyrene. In the twisted excited state (S_1), the HOMO localizes on DMA and the LUMO remains on pyrene, producing donor-to-acceptor charge transfer

TDDFT calculations (Table I) predict a single optically allowed $S_0 \rightarrow S_1$ transition at 2.93 eV (423 nm), largely unaffected by solvent polarity. This agrees with the experiment, where absorption maxima remain constant across solvents [17]. Such solvent invariance of absorption is a hallmark of LE–TICT systems like DMABN [26], where ground-state polarity has little effect on vertical excitation. By contrast, fluorescence exhibits solvent dependence. Computed S_1 emission decreases from ~1.60 eV in the gas phase to ~1.47 eV in DMSO, which is slightly lower than the experimental redshifts of ~0.5 eV [[15], [16], [26]]. This magnitude of solvatochromism is comparable to DMABN (0.4–0.6 eV across nonpolar to polar solvents [5]) and DMA-substituted chalcones (0.5–0.7 eV [3]). The trend clearly indicates stabilization of the charge-separated TICT state in polar environments, consistent with the increase in molecular dipole moment upon donor twisting.

Table 1. TDDFT findings for the gas phase and diverse solvents compared with experimental data.

Solvent	**Calculations**		**Experiment [23]**	
	E_{abs} (eV)	E_{Fluo} (eV)	E_{abs} (eV)	E_{fluo} (eV)
Gas phase	2.93	1.60	-	**-**
Cyclohexane (ε_r=2.02)	2.93	-	~2.93	~2.53
Toluene (ε_r=2.38)	2.93	1.50	~2.93	~2.38
Chloroform (ε_r=4.81)	2.93	1.52	~2.93	~2.29
THF (ε_r=7.58)	2.93	1.46	~2.93	~2.17
Acetone (ε_r=20.7)	2.93	1.49	~2.93	~2.07
DMSO (ε_r=46.8)	2.93	1.47	~2.93	~2.00

Mechanistically, solvent molecules reorganize around the charge-separated state, lowering its energy and producing a bathochromic shift (Figures 5b–d). This dielectric stabilization arises primarily from electrostatic screening of the donor–acceptor dipole by the surrounding medium. In low-polarity solvents such as cyclohexane or toluene ($\varepsilon_r < 3$), the energy gap between the LE and TICT states remains small, resulting in weakly shifted emission. In contrast, highly polar solvents such as acetone and DMSO ($\varepsilon_r > 20$) significantly stabilize the TICT configuration, giving rise to the observed redshift in fluorescence. Beyond the bulk dielectric response, specific solute–solvent interactions—hydrogen bonding, dipole alignment, or π-π stacking may further modify the excited-state landscape. These effects are not fully captured by the continuum model used here but can substantially influence the relaxation dynamics and emission wavelength [12]. Similar solvent-mediated stabilization has been reported in nitroaromatic and cyanoacrylate-based push–pull chromophores, where the polarity and hydrogen-bonding capacity of the solvent directly tune the emission [14]. Thus, StyPy fits squarely within the broader family of polarity-sensitive TICT fluorophores [12]. Small deviations between the calculated and experimental shifts may therefore reflect specific solvent–solute interactions beyond the scope of dielectric models [12,27-28]. In addition, the computed fluorescence energies are systematically underestimated compared with experiment, which is consistent with the well-known tendency of PBE-based TDDFT functionals to underestimate charge-transfer excitations due to the intrinsic delocalization error [29]. Nevertheless, the relative ordering of excitation energies across solvents is in excellent agreement with experimental observations [9,30], confirming the reliability of the computed solvent-dependent trends.

This result indicates that solvent polarity plays a crucial role in regulating the emission behavior of StyPy. In nonpolar solvents, fluorescence mainly comes from the locally excited planar structure, where the donor and acceptor parts remain strongly connected. As the solvent polarity increases, the surrounding medium stabilizes the charge-separated form, making the twisted TICT state the main source of emission. The balance between molecular relaxation and solvent stabilization determines the optical response of StyPy, confirming its behavior as a typical donor–acceptor molecule sensitive to changes in solvent polarity.

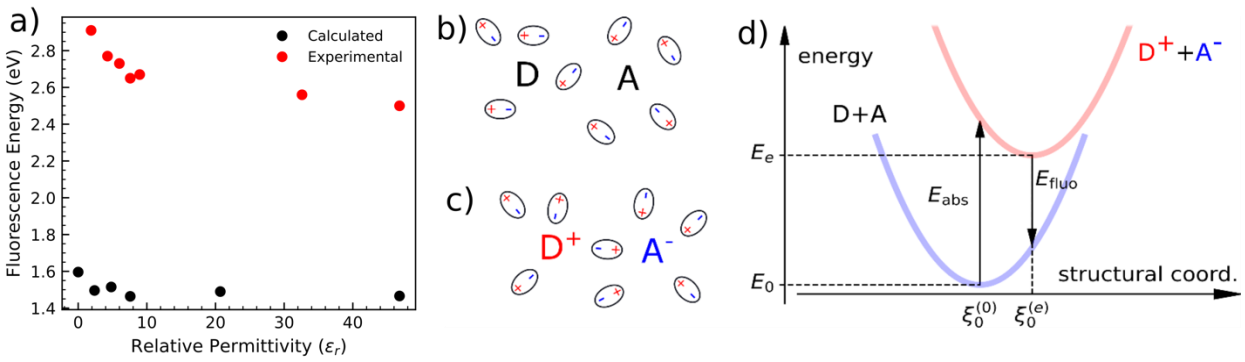

Figure 5. a) Calculated fluorescence energies of StyPy in solvents of increasing polarity, showing a systematic redshift consistent with experiment. (b–d) Representative solvent stabilization of the twisted S_1 state, where charge separation increases dipole moment and lowers emission energy.

Conclusion

StyPy undergoes TICT exclusively through rotation of the DMA donor, while the rigid PFS acceptor remains locked in conjugation with the pyrene core. The potential energy surface reveals that PFS twisting is hindered by an energy barrier of approximately 0.8 eV, whereas DMA rotation occurs on a barrierless surface, enabling ultrafast relaxation toward the twisted charge-transfer geometry. Solvent polarity further enhances this stabilization, producing a calculated fluorescence redshift in close agreement with the experimental shift. This donor-controlled pathway produces a stabilized, polar excited state, defining StyPy as part of the donor-driven TICT family. Its structural asymmetry eliminates competing torsional modes, demonstrating that rigidifying one partner in a donor–acceptor pair can enforce predictable excited-state dynamics. This design principle provides a practical route for tailoring charge-transfer emission, with implications for molecular probes, optoelectronic devices, and photonic materials. Future work will extend these findings by incorporating explicit solvent models, hybrid functionals, and ultrafast spectroscopy to validate the predicted torsional dynamics.

Acknowledgment

We express our gratitude for the computing resources supplied by the state of Baden-Württemberg via bwHPC, the Mahameru HPC at the National Research and Innovation Agency (BRIN), and the German Research Foundation (DFG) through grant no. INST 39/963-1 FUGG (bwForClusters NEMO and JUSTUS2).

References

[1] I. Borges, E. Uhl, L. Modesto-Costa, A. J. A. Aquino, and H. Lischka, "Insight into the Excited State Electronic and Structural Properties of the Organic Photovoltaic Donor Polymer Poly(thieno[3,4-b] thiophene benzodithiophene) by Means of ab Initio and Density Functional Theory," *Journal of Physical Chemistry C*, vol. 120, no. 38, pp. 21818–21826, 2016.

[2] I. Borges, A. A. J. Aquino, A. Koehn, W. L. Hase, H. Lischka, and L. X. Chen, "states in organic semiconductors for high-performance solar cells: the PTB1 / PCBM low band gap system. Ab initio modeling of excitonic and charge-transfer states in organic semiconductors: the

PTB1 / PCBM low band gap system," *Journal of American Chemical Society*, vol. 135, p. 18252−18255, 2013.

[3] R. Ghosh and D. K. Palit, "Effect of Donor-Acceptor Coupling on TICT Dynamics in the Excited States of Two Dimethylamine Substituted Chalcones," *Journal of Physical Chemistry A*, vol. 119, no. 45, pp. 11128–11137, 2015.

[4] Z. R. Grabowski, K. Rotkiewicz, and W. Rettig, "Structural Changes Accompanying Intramolecular Electron Transfer: Focus on Twisted Intramolecular Charge-Transfer States and Structures," *Chem Rev*, vol. 103, no. 10, pp. 3899–4031, 2003.

[5] L. Modesto-Costa and I. Borges, "Discrete and continuum modeling of solvent effects in a twisted intramolecular charge transfer system: The 4-N, N-dimethylaminobenzonitrile (DMABN) molecule," *Spectrochim Acta A Mol Biomol Spectrosc*, vol. 201, pp. 73–81, 2018.

[6] K. Tominaga and G. C. Walker, "Femtosecond experiments on solvation dynamics of an anionic probe molecule in methanol," *J Photochem Photobiol A Chem*, vol. 87, no. 2, pp. 127–133, 1995.

[7] R. Zheng, M. Cheng, R. Ma, D. Schipper, K. Pichugin, and G. Sciaini, "Solvent effects on the intramolecular charge transfer excited state of 3CzClIPN: a broadband transient absorption study," *Phys. Chem. Chem. Phys.*, vol. 26, no. 2, pp. 1039–1045, 2024.

[8] A. Singh, M. Kumar, and V. Bhalla, "Regulating the Twisted Intramolecular Charge Transfer and Anti-heavy Atom Effect at Supramolecular Level for Favorable Photosensitizing Activity in Water," *ACS Appl Mater Interfaces*, vol. 16, no. 45, pp. 62064–62081, Nov. 2024.

[9] M. Raisch, W. Maftuhin, M. Walter, and M. Sommer, "A mechanochromic donor-acceptor torsional spring," *Nat Commun*, vol. 12, no. 1, pp. 1–10, 2021.

[10] R. Hertel, W. Maftuhin, M. Walter, and M. Sommer, "Conformer Ring Flip Enhances Mechanochromic Performance of ansa-Donor-Acceptor-Donor Mechanochromic Torsional Springs," *J Am Chem Soc*, 2022.

[11] A. J. Reuss, C. Grünewald, H. Gustmann, J. W. Engels, and J. Wachtveitl, "Three-State Fluorescence of a 2-Functionalized Pyrene-Based RNA Label," *Journal of Physical Chemistry B*, vol. 121, no. 14, pp. 3032–3041, 2017.

[12] A. M. El-Zohry, E. A. Orabi, M. Karlsson, and B. Zietz, "Twisted Intramolecular Charge Transfer (TICT) Controlled by Dimerization: An Overlooked Piece of the TICT Puzzle," *Journal of Physical Chemistry A*, vol. 125, no. 14, pp. 2885–2894, Apr. 2021.

[13] S. Lee, M. Jen, T. Jang, G. Lee, and Y. Pang, "Twisted intramolecular charge transfer of nitroaromatic push–pull chromophores," *Sci Rep*, vol. 12, no. 1, Dec. 2022.

[14] A. Pounder, M. Pavlovic, D. Chow, A. Chen, R. A. Manderville, and S. D. Wetmore, "Photobasicity-Triggered Twisted Intramolecular Charge Transfer of Push-Pull Chromophores." Jun. 09, 2025.

[15] S. Ludwanowski, D. Hoenders, K. Kalayci, H. Frisch, C. Barner-Kowollik, and A. Walther, "Modular functionalization and hydrogel formation via red-shifted and self-reporting [2+2] cycloadditions," *Chemical Communications*, pp. 2–5, 2021.

[16] S. Sasaki, S. Suzuki, K. Igawa, K. Morokuma, and G. I. Konishi, "The K-Region in Pyrenes as a Key Position to Activate Aggregation-Induced Emission: Effects of Introducing Highly

Twisted N,N-Dimethylamines," *Journal of Organic Chemistry*, vol. 82, no. 13, pp. 6865–6873, 2017.

[17] J. J. Mortensen *et al.*, "GPAW: An open Python package for electronic structure calculations," *Journal of Chemical Physics*, vol. 160, no. 9, Mar. 2024.

[18] J. Enkovaara *et al.*, "Electronic structure calculations with GPAW: A real-space implementation of the projector augmented-wave method," *Journal of Physics Condensed Matter*, vol. 22, no. 25, 2010.

[19] M. Ernzerhof and G. E. Scuseria, "Assessment of the Perdew-Burke-Ernzerhof exchange-correlation functional," vol. 110, no. 11, pp. 5029–5036, Mar. 1999.

[20] M. E. Casida, "Time-Dependent Density Functional Response Theory for Molecules," *World Scientific*, pp. 155–192, 1995.

[21] M. Walter *et al.*, "Time-dependent density-functional theory in the projector augmented-wave method," *Journal of Chemical Physics*, vol. 128, no. 24, 2008.

[22] A. Held and M. Walter, "Simplified continuum solvent model with a smooth cavity based on volumetric data," *Journal of Chemical Physics*, vol. 141, no. 17, 2014.

[23] S. Ludwanowski, A. Samanta, S. Loescher, C. Barner-Kowollik, and A. Walther, "A Modular Fluorescent Probe for Viscosity and Polarity Sensing in DNA Hybrid Mesostructures," *Advanced Science*, vol. 8, no. 5, Mar. 2021.

[24] Z. He, R. Xue, Y. Lei, L. Yu, and C. Zhu, "Photorelaxation pathways of 4-(N,N-dimethylamino)-4′-nitrostilbene upon S1 excitation revealed by conical intersection and intersystem crossing networks," *Molecules*, vol. 25, no. 9, May 2020.

[25] S. Thekku Veedu, D. Raiser, R. Kia, M. Scholz, and S. Techert, "Ultrafast dynamical study of pyrene-N,N-dimethylaniline (PyDMA) as an organic molecular diode in solid state," *Journal of Physical Chemistry B*, vol. 118, no. 12, pp. 3291–3297, 2014.

[26] P. B. Coto, L. Serrano-Andrés, T. Gustavsson, T. Fujiwara, and E. C. Lim, "Intramolecular charge transfer and dual fluorescence of 4-(dimethylamino) benzonitrile: Ultrafast branching followed by a two-fold decay mechanism," *Physical Chemistry Chemical Physics*, vol. 13, no. 33, pp. 15182–15188, Sep. 2011.

[27] H. Lischka *et al.*, "Multireference Approaches for Excited States of Molecules," *Chemical Reviews*, vol. 118, no. 15. American Chemical Society, pp. 7293–7361, Aug. 08, 2018.

[28] L. González, D. Escudero, and L. Serrano-Andrés, "Progress and challenges in the calculation of electronic excited states," *ChemPhysChem*, vol. 13, no. 1. Wiley-VCH Verlag, pp. 28–51, Jan. 16, 2012.

[29] A. J. Cohen, P. Mori-Sánchez, and W. Yang, "Insights into current limitations of density functional theory," *Science (1979)*, vol. 321, no. 5890, pp. 792–794, 2008.

[30] R. Wessling *et al.*, "Phenothiazine-Based Donor-Acceptor Polymers as Multifunctional Materials for Charge Storage and Solar Energy Conversion," *Macromol Rapid Commun*, vol. 2200699, p. 2200699, 2022.